Proceedings of the 17th World Congress
The International Federation of Automatic Control
Seoul, Korea, July 6-11, 2008

# Coordinated Path Following of Multiple UAVs for Time-Critical Missions in the Presence of Time-Varying Communication Topologies ⋆

**A. P. Aguiar** * **I. Kaminer** ** **R. Ghabcheloo** * **A. M. Pascoal** *
**E. Xargay** *** **N. Hovakimyan** *** **C. Cao** *** **V. Dobrokhodov** **

* *Institute for Systems and Robotics (ISR), Instituto Superior Técnico (IST), Lisbon, Portugal e-mail: {pedro,reza,antonio}@isr.ist.utl.pt*
** *Naval Postgraduate School, Monterey, CA 93943, e-mail: {kaminer,vldobr}@nps.edu*
*** *Aerospace & Ocean Engineering, Virginia Polytechnic Institute & State University, Blacksburg, VA 24061, e-mail: {xargay, nhovakim, chengyu}@vt.edu*

**Abstract:** We address the problem of steering multiple unmanned air vehicles (UAVs) along given paths (path-following) under strict temporal coordination constraints requiring, for example, that the vehicles arrive at their final destinations at exactly the same time. Path-following relies on a nonlinear Lyapunov based control strategy derived at the kinematic level with the augmentation of existing autopilots with $\mathcal{L}_1$ adaptive output feedback control laws to obtain inner-outer loop control structures with guaranteed performance. Multiple vehicle time-critical coordination is achieved by enforcing temporal constraints on the speed profiles of the vehicles along their paths in response to information exchanged over a dynamic communication network. We consider that each vehicle transmits its coordination state to only a subset of the other vehicles, as determined by the communications topology adopted. We address explicitly the case where the communication graph that captures the underlying communication network topology may be disconnected during some interval of time (or may even fail to be connected at any instant of time) and provide conditions under which the closed-loop system is stable. Flight test results obtained at Camp Roberts, CA in 2008 and hardware-in-the-loop (HITL) simulations demonstrate the benefits of the algorithms developed.

Keywords: Coordinated path following; Multiple UAVs; Dynamic communication networks.

## 1. INTRODUCTION

Unmanned Aerial Vehicles (UAVs) are becoming ubiquitous and play an ever increasing role in a number of missions that include military reconnaissance and strike operations, border patrol missions, forest fire detection, and police surveillance and recovery operations. In a typical application, a single autonomous vehicle is managed by a crew using a ground station provided by the vehicle manufacturer. To execute more challenging missions, however, requires the use of multiple vehicles working together to achieve a common objective. Representative examples of cooperative mission scenarios are sequential auto-landing and coordinated ground target suppression for multiple UAVs. The first refers to the situation where a fleet of UAVs must break up and arrive at the assigned glideslope point, separated by pre-specified safe-guarding time-intervals. In the case of ground target suppression, a formation of UAVs must again break up and execute a coordinated maneuver to arrive at a predefined position over the target at the same time. In both cases, no absolute temporal constraints are given *a priori* - a critical point that needs to be emphasized. Furthermore, the vehicles must execute maneuvers in close proximity to each other. As pointed out in [Kaminer et al. 1998, Kim and Mesbahi 2006], the flow of information among vehicles may be severely restricted, either for security reasons or because of tight bandwidth limitations. As a consequence, no vehicle will be able to communicate with the entire formation and the inter-vehicle communication network may change over time. It is therefore imperative to develop coordinated motion control strategies that can yield robust performance in the presence of communication failures and switching communication topologies.

Motivated by these and similar problems, there has been over the past few years a flurry of activity in the area of multi-agent system networks with application to engineering and science problems. The range of topics addressed include parallel computing [Tsitsiklis and Athans 1984], synchronization of oscillators [Sepulchre et al. 2003], study of collective behavior and flocking [Jadbabaie et al. 2003], multi-system consensus mechanisms [Lin et al. 2005], multi-vehicle system formations [Egerstedt and Hu 2001], coordinated motion control [Ghabcheloo et al. 2006b], asynchronous protocols [Fang et al. 2005], dynamic graphs [Mesbahi 2005], stochastic graphs [Mesbahi

⋆ Research supported in part by projects GREX / CEC-IST (Contract No. 035223), NAV-Control / FCT-PT (PTDC/EEA-ACR/65996/2006), FREESUBNET RTN of the CEC, the FCT-ISR/IST plurianual funding program through the POS_C Program that includes FEDER funds, USSOCOM, ONR under Contract N00014-05-1-0828, AFOSR under Contract No. FA9550-05-1-0157, and ARO under Contract No. W911NF-06-1-0330

2005, Stilwell and Bishop 2000, Stilwell et al. 2006], and graph-related theory [Cao et al. 2005, Kim and Mesbahi 2006]. Especially relevant are the applications of the theory developed in the area of multi-vehicle formation control: spacecraft formation flying [Mesbahi and Hadaegh 2001], unmanned aerial vehicle (UAV) control [Song et al. 2005, Stipanovic et al. 2004], coordinated control of land robots [Ghabcheloo et al. 2006b], and control of multiple autonomous underwater vehicles (AUVs) [Ghabcheloo et al. 2006a, Aguiar and Pascoal 2007].

In [Kaminer et al. 2007], a general framework for the problem of coordinated control of multiple autonomous vehicles that must operate under strict spatial and temporal constraints was presented. The proposed framework borrows from multiple disciplines and integrates algorithms for path generation, path following, time-critical coordination, and $\mathcal{L}_1$ adaptive control theory for fast and robust adaptation. Together, these techniques yield control laws that meet strict performance requirements in the presence of modeling uncertainties and environmental disturbances. The methodology proposed in [Kaminer et al. 2007] is exemplified for the case of UAVs and unfolds in three basic steps. First, given a multiple vehicle task, a set of feasible trajectories is generated for all UAVs using a direct method of calculus of variations that takes explicitly into account the initial and final boundary conditions, a general performance criterion to be optimized, the simplified UAV dynamics, and safety rules for collision avoidance. The second step consists of making each vehicle follow its assigned path while tracking a desired speed profile. Path following control design is first done at a kinematic level, leading to an outer-loop controller that generates pitch and yaw rate commands to an inner-loop controller. The latter relies on off-the-shelf autopilots for angular rate command tracking, augmented with an $\mathcal{L}_1$ adaptive output feedback control law that guarantees stability and performance of the complete system for each vehicle in the presence of modeling uncertainties and environmental disturbances. Finally, in the third step the speed profile of each vehicle is adjusted to enforce the temporal constraints that must be met in order to coordinate the entire fleet of UAVs. This step relies on the underlying communication network as a means of information exchange between the vehicles.

This paper builds upon and complements the results in [Kaminer et al. 2007] to deal with network communication failures. In particular, we address explicitly the case where the communication graph that captures the underlying communication network topology may be disconnected during some interval of time or may even fail to be connected at any instant of time. Flight test results and hardware-in-the-loop (HITL) simulations demonstrate the benefits of the algorithms developed. More flight tests are planned at Camp Roberts, CA in April-May 2008.

Due to space limitations, all the proofs are omitted.

## 2. PATH FOLLOWING IN 3D SPACE

This section formulates the problem of path following control for a (single) UAV in 3D space. We recall that *path following* refers to the problem of making a vehicle converge to and follow a desired feasible path. Although in general no time schedule is assigned to the path, one may assign a desired speed profile for the vehicle to track.

In what follows we avail ourselves of the results derived in [Kaminer et al. 2006] (see also [Taranenko 1986, Yakimenko 2000]) where an algorithm was proposed to generate space deconflicting feasible paths for multiple UAVs, that is, paths that do not intersect each other and that yield trajectories that can be tracked by an UAV without exceeding prespecified bounds on its velocity and total acceleration along that trajectory.

In order for the $i$th vehicle to follow the spatial path $p_{c_i}$ using the algorithm in [Kaminer et al. 2006], a path following algorithm that extends the one in [Soetanto et al. 2003] to a 3D setting with a further modification aimed at meeting time-critical and inter-vehicle constraints is now presented. At this level, only the simplified kinematic equations of the vehicle are addressed. The dynamics of the closed-loop UAV with autopilot are dealt with in Sections 5 and 6 by introducing an inner-loop control law via a novel $\mathcal{L}_1$ adaptive output feedback controller.

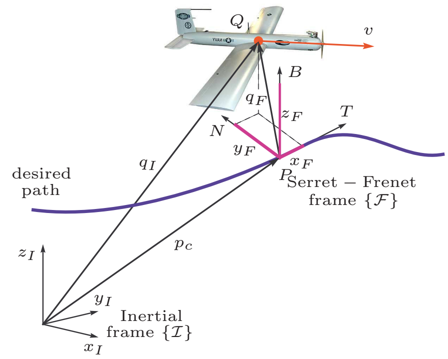


Fig. 1. Problem geometry

The required notation is introduced with reference to Figure 1. Let $\mathcal{I}$ denote an inertial frame. Let $Q$ be the UAV center of mass and $\mathcal{W}$ be the wind frame attached to the UAV. Further, let $p_c(l)$ be the path to be followed, parameterized by its path length $l$, and let $P$ be an arbitrary point on the path that plays the role of the center of mass of a virtual UAV to be followed. Let $\mathcal{F}$ be a Serret-Frenet frame attached to the point $P$ on the path, and let $T(l)$, $N(l)$ and $B(l)$ present an orthonormal basis for $\mathcal{F}$. Note that these unit vectors define the tangent, normal, and binormal directions, respectively, to the path at the point determined by $l$. Finally, let

$$q_F(t) = [\, x_F(t) \;\; y_F(t) \;\; z_F(t) \,]^\top$$

be the position of the UAV center of mass $Q$ with respect to the Frenet frame resolved in $\mathcal{F}$, and let

$$\Phi_e(t) = [\, \phi_e(t) \;\; \theta_e(t) \;\; \psi_e(t) \,]^\top$$

denote the Euler angles that locally parameterize the rotation matrix from $\mathcal{F}$ to $\mathcal{W}$.

In what follows, $v(t)$ is the magnitude of the UAV's velocity vector, and $q(t)$ and $r(t)$ are the $x$-axis and $z$-axis components, respectively, of the vehicle's rotational velocity resolved in wind frame $\mathcal{W}$. With a slight abuse of notation, $q(t)$ and $r(t)$ will be referred to as *pitch rate* and *yaw rate*, respectively, in the wind frame $\mathcal{W}$.

Straightforward computations [1] yield the dynamic equations of the path following kinematic error states as:

[1] See [Kaminer et al. 2006] for details in the derivation of these dynamics.

$$\mathcal{G}_e : \begin{cases} \dot{x}_F = -\dot{l}(1-\kappa(l)y_F) + v\cos\theta_e\cos\psi_e \\ \dot{y}_F = -\dot{l}(\kappa(l)x_F - \zeta(l)z_F) + v\cos\theta_e\sin\psi_e \\ \dot{z}_F = -\dot{l}\zeta(l)y_F - v\sin\theta_e \\ \begin{bmatrix}\dot{\theta}_e \\ \dot{\psi}_e\end{bmatrix} = D(t,\theta_e,\psi_e) + T(t,\theta_e)\begin{bmatrix} q \\ r\end{bmatrix} \end{cases} \tag{1}$$

where

$$D(t,\theta_e,\psi_e) = \begin{bmatrix} \dot{l}\zeta(l)\sin\psi_e \\ -\dot{l}(\zeta(l)\tan\theta_e\cos\psi_e + \kappa(l)) \end{bmatrix}$$

$$T(t,\theta_e) = \begin{bmatrix} \cos\phi_e & -\sin\phi_e \\ \frac{\sin\phi_e}{\cos\theta_e} & \frac{\cos\phi_e}{\cos\theta_e} \end{bmatrix},$$

and $\kappa(l)$ and $\zeta(l)$ are the curvature and the torsion of the path respectively. Note that, in the kinematic error model (1), $q(t)$ and $r(t)$ play the role of control inputs. Notice also how $\dot{l}(t)$ becomes an extra variable that can be manipulated at will.

Furthermore, we define the state vector for the path following kinematic dynamics as:

$$x(t) = [\, x_F(t)\ \ y_F(t)\ \ z_F(t)\ \ \theta_e(t) - \delta_\theta(t)\ \ \psi_e(t) - \delta_\psi(t)\,]^\top,$$

where

$$\delta_\theta = \sin^{-1}\left(\frac{z_F}{|z_F| + d_1}\right), \qquad \delta_\psi = \sin^{-1}\left(\frac{y_F}{|y_F| + d_2}\right),$$

with $d_1$ and $d_2$ some positive constants. Notice that, instead of the angular errors $\theta_e(t)$ and $\psi_e(t)$, we use $\theta_e(t) - \delta_\theta(t)$ and $\psi_e(t) - \delta_\psi(t)$ respectively to shape the "approach" angles to the path. The system $\mathcal{G}_e$ is completely characterized by defining the vector of input signals as:

$$y(t) = [\, q(t)\ \ r(t)\,]^\top.$$

Next, we show that there exist stabilizing functions for $q(t)$ and $r(t)$ leading to local exponential stability of the origin of $\mathcal{G}_e$ with a prescribed domain of attraction. We start by assuming that the UAV speed satisfies the lower bound

$$v(t) \geq v_{\min}, \qquad \forall\, t \geq 0. \tag{2}$$

Furthermore, let $c_1$ and $c_2$ be arbitrary positive constants satisfying the following condition

$$\nu_i \triangleq \sqrt{cc_2} + \sin^{-1}\left(\frac{\sqrt{cc_1}}{\sqrt{cc_1} + d_i}\right) \ \leq\ \frac{\pi}{2} - \epsilon_i, \quad i = 1,2$$

where $c > 0$ is any positive constant, $d_1$ and $d_2$ were introduced in (1), and $\epsilon_1$ and $\epsilon_2$ are positive constants such that $0 < \epsilon_i < \frac{\pi}{2}$, $i = 1,2$. Letting the progression of the point $P$ along the path be governed by

$$\dot{l}(t) = k_1 x_F(t) + v(t)\cos\theta_e(t)\cos\psi_e(t), \tag{3}$$

where $k_1 > 0$, the functions

$$\begin{bmatrix} q_c \\ r_c \end{bmatrix} = T^{-1}(t,\theta_e)\left(\begin{bmatrix} u_{\theta_c} \\ u_{\psi_c}\end{bmatrix} - D(t,\theta_e,\psi_e)\right), \tag{4}$$

where $u_{\theta_c}(t)$ and $u_{\psi_c}(t)$ are defined as:

$$\begin{aligned} u_{\theta_c} &= -k_2(\theta_e - \delta_\theta) \\ &\quad + \frac{c_2}{c_1} z_F v \frac{\sin\theta_e - \sin\delta_\theta}{\theta_e - \delta_\theta} + \dot{\delta}_\theta \\ u_{\psi_c} &= -k_3(\psi_e - \delta_\psi) \\ &\quad - \frac{c_2}{c_1} y_F v\cos\theta_e \frac{\sin\psi_e + \sin\delta_\psi}{\psi_e - \delta_\psi} + \dot{\delta}_\psi, \end{aligned} \tag{5}$$

stabilize the subsystem $\mathcal{G}_e$ for any $k_2 > 0$ and $k_3 > 0$.

*Lemma 1.* Let the progression of the point $P$ along the path be governed by (3). Then, for any $v(t)$ verifying (2), the origin of the kinematic error equations in (1) with the controllers $q(t) \equiv q_c(t)$, $r(t) \equiv r_c(t)$ defined in (4)-(5) is exponentially stable with the domain of attraction

$$\Omega = \left\{ x \ :\ V_p(x) < \frac{c}{2} \right\}, \tag{6}$$

$$V_p(x) = x^\top \bar{P} x, \quad \bar{P} = \operatorname{diag}\left(\frac{1}{2c_1}, \frac{1}{2c_1}, \frac{1}{2c_1}, \frac{1}{2c_2}, \frac{1}{2c_2}\right). \square$$

## 3. TIME-CRITICAL COORDINATION

We now address the problem of time-coordinated control of multiple UAVs. Examples of applications in which this would be useful include situations where all vehicles must arrive at their final destinations at exactly the same time, or at different times so as to meet a desired inter-vehicle arrival schedule. Without loss of generality, we consider the problem of simultaneous arrival. Let $t_f$ be the arrival time of the first UAV. Denote $l_{f_i}$ as the total length of the spatial path for the $i$th UAV. In addition, let $l_i(t)$ be the path length from the origin to $p_{c_i}(t)$ along the spatial path of the $i$th UAV. Define $l'_i(t) = l_i(t)/l_{fi}$. Clearly, $l'_i(t_f) = 1$ for $i = 1, 2, \ldots, n$ implies that all vehicles arrive at their final destination at the same time. Since $\dot{l}'_i(t) = \dot{l}_i(t)/l_{fi}$, it follows from (3) that

$$\dot{l}'_i(t) = \frac{k_1 x_{F_i}(t) + v_i(t)\cos\theta_{e,i}(t)\cos\psi_{e,i}(t)}{l_{fi}}. \tag{7}$$

To account for the communication constraints, we introduce the neighborhood set $J_i$ that denotes the set of vehicles that the $i$th vehicle exchanges information with. We impose the constraint that each UAV only exchanges its coordination parameter $l'_i(t)$ with its neighbors according to the topology of the communication network.

To solve the coordination problem, we propose the following desired speed profile for the $i$th UAV [Kaminer et al. 2006]

$$v_{c_i} = \frac{u_{\text{coord}_i} l_{fi} - k_1 x_{F_i}}{\cos\theta_{e,i}\cos\psi_{e,i}}, \quad i = 1, \ldots, n, \tag{8}$$

with the following decentralized coordination law

$$\begin{aligned} u_{\text{coord},1} &= -a\sum_{j\in J_1}(l'_1 - l'_j) + \frac{v_{d,1}}{l_{f_1}} \\ u_{\text{coord},i} &= -a\sum_{j\in J_i}(l'_i - l'_j) + \chi_{I,i}, \qquad i = 2,\ldots,n \\ \dot{\chi}_{I,i} &= -b\sum_{j\in J_i}(l'_i - l'_j), \qquad\qquad i = 2,\ldots,n \end{aligned}$$

where we have elected vehicle 1 as the leader, $v_{d,1}(t)$ denote its desired speed profile, and $a$, $b$ are positive constants. Note that the coordination control law has a Proportional-Integral structure, thus allowing each vehicle to learn the speed of the leader, rather than having it available *a priori*.

The coordination law can be rewritten in compact form as:

$$u_{\text{coord}}(t) = -aL(t)l'(t) + \begin{bmatrix} v_{d,1}(t)/l_{f_1} \\ \chi_I(t) \end{bmatrix}, \tag{9}$$

$$\dot{\chi}_I(t) = -bCL(t)l'(t), \tag{10}$$

where $l'(t) = [l'_1(t) \;\ldots\; l'_n(t)]^\top$, $u_{\rm coord}(t) = [u_{{\rm coord}_1}(t) \;\ldots\; u_{{\rm coord}_n}(t)]^\top$, $\chi_I(t) = [\chi_{I,2}(t) \;\ldots\; \chi_{I,n}(t)]^\top$, $C = [\,0 \;\; I_{n-1}\,]$, and the $n \times n$ piecewise-continuous matrix $L(t)$ can be interpreted as the Laplacian of an undirected graph $\Gamma(t)$ that captures the underlying bidirectional communication network topology of the UAV formation at time $t$. It is well known that $L^\top = L$, $L \geq 0$, $L1_n = 0$, and that the second smallest eigenvalue of $L$ is strictly positive if and only if the graph $\Gamma$ is connected (see e.g., [Biggs 1993]).

Next we reformulate the coordination problem stated above as a stabilization problem. To this aim, we introduce the following notation. Let

$$\Pi \triangleq I_n - \frac{1_n 1_n^\top}{n},$$

and let $Q$ be a $(n-1) \times n$ matrix such that

$$Q1_n = 0, \quad QQ^\top = I_{n-1}.$$

Notice that $Q^\top Q = \Pi$, $\Pi = \Pi^\top = \Pi^2 > 0$, $L\Pi = \Pi L = L$, and the spectrum of the matrix $\bar{L} \triangleq QLQ^\top$ is equal to the spectrum of $L$ without the eigenvalue $\lambda = 0$ correspondent to the eigenvector $1_n$. Define the state variables $\zeta(t) = \left[\zeta_1(t)^\top \; \zeta_2(t)^\top\right]^\top$ as:

$$\zeta_1(t) = Q\, l'(t)\,, \qquad \zeta_2(t) = \chi_I(t) - \frac{v_{d,1}(t)}{l_{f_1}} 1_{n-1}\,,$$

where by definition $\zeta_1(t) = 0 \Leftrightarrow l' \in \text{span}\{1_n\}$ which implies that, if $\zeta(t_f) = 0$, then all UAVs arrive at their final destination at the same time.

Thus, denoting the velocity error for the $i$th vehicle in the coordination by $\tilde{v}_i(t) = v_i(t) - v_{c_i}(t)\,,\; i = 1, \ldots, n$, the closed-loop coordination dynamics formed by (7) and (8)-(10) can be reformulated as:

$$\dot{\zeta}(t) = F(t)\zeta(t) + G\dot{v}_{d,1}(t) + H\varphi(t)\,, \tag{11}$$

where

$$F(t) = \begin{bmatrix} -a\bar{L}(t) & QC \\ -bC^\top Q^\top \bar{L}(t) & 0 \end{bmatrix}$$

$$G = \frac{1}{l_{f_1}} \begin{bmatrix} 0 \\ -I \end{bmatrix} \qquad H = \begin{bmatrix} Q \\ 0 \end{bmatrix},$$

and $\varphi(t) \in \mathbb{R}^n$ is a vector with its $i$th element $\frac{\tilde{v}_i(t)\cos\theta_{e,i}(t)\cos\psi_{e,i}(t)}{l_{fi}}$.

Next we show that for fixed or time-varying communication topologies, but assuming that the graph remains connected for all $t \geq 0$, if every vehicle travels at the desired speed $v_{c_i}(t)$ and the speed profile of the leader $v_{d,1}$ is constant, then the coordinated system reaches agreement and all the vehicles travel at the same path-length rate. However, if $v_{d,1}(t)$ is not constant but its time-derivative $\dot{v}_{d,1}(t)$ is bounded, then the error of the disagreement vector $\zeta_1(t)$ degrades gracefully with the size of $\dot{v}_{d,1}(t)$.

*Lemma 2.* Consider the coordination system (11) and suppose that the graph that models the communication topology $\Gamma(t)$ is connected for all $t \geq 0$. Then, for any selected rate of convergence $\lambda > 0$, there exist a sufficiently large coordinated control gains $a, b$ such that the system (11) is input-to-state stable (ISS) with respect to $\dot{v}_{d,1}(t)$ and $\tilde{v}(t) = [\tilde{v}_1, \ldots, \tilde{v}_n]^\top$, that is,

$$\begin{aligned} \|\zeta(t)\| \leq k_1 \|\zeta(0)\| e^{-\lambda t} + k_2 \sup_{\tau\in[0,t)} |\dot{v}_{d,1}(\tau)| \\ + k_3 \sup_{\tau\in[0,t)} \|\tilde{v}(\tau)\|\,, \quad \forall t \geq 0 \end{aligned} \tag{12}$$

for some $k_1, k_2, k_3 > 0$. Furthermore, the normalized lengths $l'_i(t)$ and path-length rates $\dot{l}'_i(t)$ satisfy

$$\begin{aligned} \lim_{t\to\infty} \sup \left| l'_i(t) - l'_j(t) \right| \leq k_4 \lim_{t\to\infty} \sup |\dot{v}_{d,1}(t)| \\ + k_5 \lim_{t\to\infty} \sup \|\tilde{v}(t)\|\,, \end{aligned} \tag{13}$$

$$\begin{aligned} \lim_{t\to\infty} \sup \left| \dot{l}'_i(t) - \frac{v_{d,1(t)}}{l_{f_1}} \right| \leq k_6 \lim_{t\to\infty} \sup |\dot{v}_{d,1}(t)| \\ + k_7 \lim_{t\to\infty} \sup \|\tilde{v}(t)\|\,, \end{aligned} \tag{14}$$

for all $i, j \in \{1, \ldots, n\}$, and for some $k_4, k_5, k_6, k_7 > 0$. □

We now consider the case where the communication graph $\Gamma(t)$ may be disconnected during some interval of time or may even fail to be connected at any instant of time; however, we assume that the connectivity of the graph satisfies the following less restrictive persistency of excitation (PE)-like condition

$$\frac{1}{T}\int_t^{t+T} x^\top \bar{L}(\tau) x d\tau \geq \bar{\mu}, \qquad \forall t \geq 0\,; \;\; \forall x \in \mathbb{R}^{n-1} \tag{15}$$

for some $T, \bar{\mu} > 0$.

*Lemma 3.* Consider the coordination system (11) and suppose that the Laplacian of the graph that models the communication topology satisfies the PE condition (15). Then, for any given $\lambda > 0$ there exist sufficiently large coordination control gains $a, b$ such that the system (11) is ISS with respect to $\dot{v}_{d,1}(t)$ and $\tilde{v}(t)$. Moreover, $l'_i(t)$ and $\dot{l}'_i(t)$ satisfy (13) and (14), respectively. □

*Remark 4.* The PE condition (15) only requires the graph be connected in an integral sense, not pointwise in time. Similar type of conditions for other coordination laws can be found in e.g. [Lin et al. 2007] and [Arcak 2007].

## 4. $\mathcal{L}_1$ ADAPTIVE AUGMENTATION OF COMMERCIAL AUTOPILOTS

So far, both the path following and time-critical coordination strategies have been based on the vehicle kinematics only (outer-loop control). It is now necessary to bring the UAV dynamics into play. To this effect, the above variables must be viewed as commands to be tracked by an appropriately designed inner-loop control system. At this point, a key constraint is included: the inner-loop control systems should build naturally on existent autopilots. Since commercial autopilots are normally designed to track simple way-point commands, we modify the pitch and yaw rates, as well as the speed commands computed before by including an $\mathcal{L}_1$ adaptive loop. We notice that this $\mathcal{L}_1$ augmentation is what allows us to account for the UAV dynamics.

We define now the system $\mathcal{G}_p$, which models the closed-loop system of the UAV with the autopilot, as:

$$\mathcal{G}_p : \begin{cases} v(s) = G_v(s)\left(v_{ad}(s) + z_v(s)\right) \\ q(s) = G_q(s)\left(q_{ad}(s) + z_q(s)\right) \\ r(s) = G_r(s)\left(r_{ad}(s) + z_r(s)\right) \end{cases} \tag{16}$$

where $G_v(s)$, $G_q(s)$, $G_r(s)$ are unknown strictly proper and stable transfer functions, and $z_v(t)$, $z_q(t)$, $z_r(t)$ represent bounded time-varying disturbances with uniformly bounded derivatives. We note that only very limited knowledge of the autopilot is assumed. We do not assume knowledge of the state dimension of $G_v(s)$, $G_q(s)$ and $G_r(s)$. We only assume that these are strictly proper and stable transfer functions. We nevertheless notice that the bandwidth of the control channel of the closed-loop UAV with the autopilot is very limited, and that model (16) is valid only for low-frequency approximation of $\mathcal{G}_p$. Then, since $q_c(t)$ and $r_c(t)$ defined in (4)-(5) stabilize $\mathcal{G}_e$, and $v_c(t)$ in (8) (with the coordination control algorithm (9)-(10)) leads to coordination in time, the control objective is reduced to designing an $\mathcal{L}_1$ adaptive controller $u(t) = [v_{ad}(t)\ q_{ad}(t)\ r_{ad}(t)]^\top$ such that the output $y(t) = [v(t)\ q(t)\ r(t)]^\top$ tracks the reference input $y_c(t) = [v_c(t)\ q_c(t)\ r_c(t)]^\top$ following a desired model $M(s)$, i.e.

$$y(s) \approx M(s) y_c(s) .$$

## 5. PATH FOLLOWING WITH $\mathcal{L}_1$ ADAPTIVE AUGMENTATION

We now address the stability of the path following closed-loop system with $\mathcal{L}_1$ augmentation. We show that the original domain of attraction for the kinematic error equations in (6) can be retained with the $\mathcal{L}_1$ augmentation.

*Theorem 5.* Let the progression of the point $P$ along the path be governed by (3). For any smooth $v(t)$ verifying (2), if $x(0) \in \Omega$, where $\Omega$ is defined in (6), then there exist adaptation control gains that guarantee $x(t) \in \Omega$ for all $t \geq 0$, and therefore the complete closed-loop cascaded system is ultimately bounded with the bounds as those for the kinematic closed-loop system of Lemma 1. □

*Remark 6.* We notice that the approach in this paper is different from common backstepping-type analysis for cascaded systems. The advantage of our structure is that it retains the properties of the autopilot, which is designed to stabilize the inner-loop. As a result, it leads to ultimate boundedness instead of asymptotic stability. From a practical point of view, the inner/outer-loop architecture adopted is quite versatile in that it adapts itself to the particular autopilot installed on-board.

## 6. COMBINED PATH FOLLOWING AND TIME-CRITICAL COORDINATION WITH $\mathcal{L}_1$ ADAPTIVE AUGMENTATION

This section addresses the stability properties of the combined path following/coordination systems and the inner-loop with $\mathcal{L}_1$ adaptive augmentation (see Figure 2).

*Theorem 7.* Consider the combined path following system (1) and the time-critical coordination system (11) under the communication constraints of Lemmas 2 or 3. There exist suitable control gains that guarantee that the path following errors $x(t)$ are ultimately bounded and satisfy $x(t) \in \Omega$, and that the coordination errors $\zeta(t)$ satisfy (12). Furthermore, the resulting velocity for the $i$th UAV verifies the *a priori* specified lower bound $v_i(t) \geq v_{\min} > 0$. □

## 7. EXPERIMENTAL RESULTS

The complete coordination path following control algorithm was implemented on experimental UAV RASCALs operated by NPS. The payload bay of each aircraft is used to house two PC104 embedded computers, a wireless

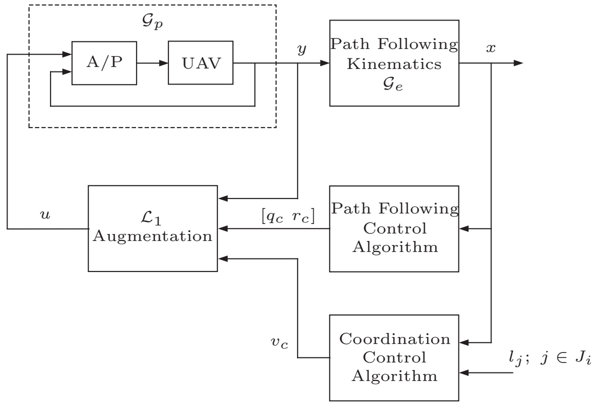


Fig. 2. Coordinated path following closed-loop for the $i$th UAV with $\mathcal{L}_1$ augmentation

network link, and the Piccolo autopilot. The first PC-104 board runs developed algorithms in real-time while directly communicating with the autopilot. The second PC-104 computer is equipped with a mesh network card that provides wireless communication to another UAV and to the ground station. This setup is being used for both hardware-in-the-loop (HITL) simulations and flight tests.

The path-following control algorithm for a single UAV was flight tested in February 2008. These flight tests demonstrated the benefits of the $\mathcal{L}_1$ adaptive augmentation to achieve improved path following performance. Figure 3(a) presents one of the trials used to tune the control parameters. In particular, it shows the inertial position of the UAV with respect to the commanded feasible trajectory. It can be seen that the maximum deviation from the desired trajectory is of about 150 m, which corresponds to the point of the sharp turn. Other than at this point, the tracking errors are very small and the UAV is following the commanded path very closely (Figure 3(b)). Moreover, the control efforts required to bring each airplane to the commanded trajectory do not exceed any limitations imposed by the autopilot and are typical for this class of UAVs.

Figures 4(a)-4(b) include results of an HITL test where two UAVs follow feasible trajectories while using their velocities to coordinate simultaneous arrival in the presence of communication failures. Figure 4(a) shows the desired and the actual paths of each UAV, while their normalized coordination states are presented in Figure 4(b). Both UAVs arrive at the final position at nearly the same time.

The results presented above demonstrate feasibility of the onboard integration of the path following, adaptation and coordination concepts. The achieved functionality of the UAV following 3D curves in inertial space has never been available for the airplanes equipped with traditional AP; the adaptive strategy outperforms the conventional waypoint navigation method. Presented results not only demonstrate the feasibility of the concept but provide a roadmap for further development and onboard implementation of intelligent multi-UAV coordination.

## 8. CONCLUSION

A novel solution was presented to the problem of coordinated control of multiple UAVs for time-critical missions in the presence of time-varying communication topologies. The framework adopted makes use of algorithms

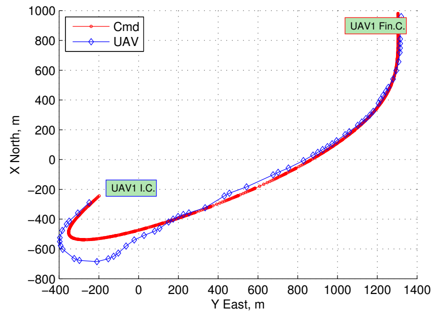


(a) UAV trajectory: 2D projection.

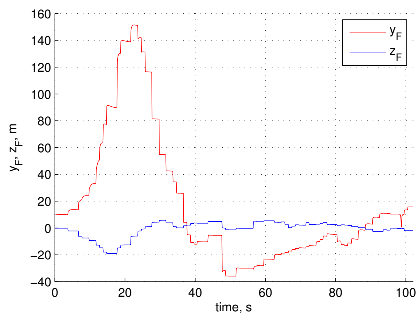


(b) Path following errors $y_F$ and $z_F$.

Fig. 3. Flight test results of path following for a single UAV.

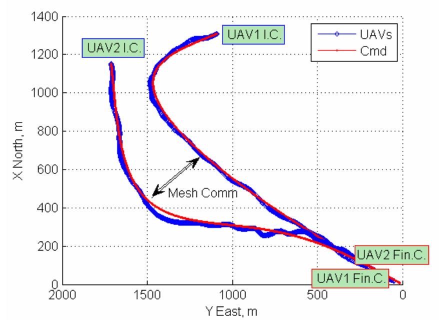


(a) UAV trajectories: 2D projection.

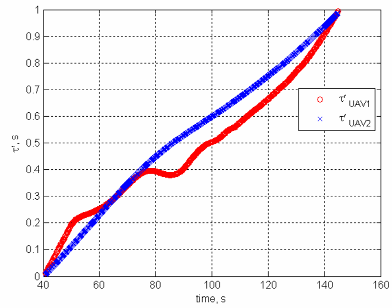


(b) Coordination states $l_i'(t)$.

Fig. 4. HITL simulation of coordinated path following for two UAVs.

for deconflicted real-time path generation, nonlinear path following, and multiple vehicle coordination. The proposed control algorithm has an inner-outer structure that relies on the augmentation of existing autopilots with $\mathcal{L}_1$ adaptive output feedback controllers. Multiple vehicle coordinated control is done by adjusting the speed profiles of the UAVs along their paths in response to information exchanged over the underlying communication network. Both theoretical and flight test results were presented.

## REFERENCES

A. P. Aguiar and A. M. Pascoal. Coordinated path-following control for nonlinear systems with logic-based communication. In *Proceedings of the $46^{th}$ IEEE Conference on Decision and Control (CDC'07)*, New Orleans, LO, USA, December 2007.

M. Arcak. Passivity as a desing tool for group coordination. *IEEE Transaction on Automatic Control*, 52(8):1380–1390, Aug 2007.

N. Biggs. *Algebraic Graph Theory.* Cambridge University Press, 1993.

M. Cao, D. Spielman, and A. Morse. A lower bound on convergence of a distributed network consensus algorithm. In *Proc. of IEEE Conf. on Decision & Control*, pages 2356–2361, Seville, Spain, 2005.

M. Egerstedt and X. Hu. Formation control with virtual leaders and reduced communications. *IEEE Trans. on Robotics and Automation*, 17(6):947–951, Dec. 2001.

L. Fang, P. Antsaklis, and A. Tzimas. Asynchronous consensus protocols: Preliminary results, simulations and open questions. In *Proc. of IEEE Conf. on Decision and Control*, pages 2194–2199, Seville, Spain, 2005.

R. Ghabcheloo, P. Aguiar, A. Pascoal, C. Silvestre, I. Kaminer, and J. Hespanha. Coordinated path following control of autonomous underwater vehicles in presence of communication failures. In *Proc. of IEEE Conf. on Decision and Control*, San Diego, CA, 2006a.

R. Ghabcheloo, A. Pascoal, C. Silvestre, and I. Kaminer. Coordinated path following control of multiple wheeled robots using linearization techniques. *International Journal of Systems Science, Taylor and Francis*, 37(6):399–414, 2006b.

A. Jadbabaie, J. Lin, and A. Morse. Coordination of groups of mobile autonomous agents using nearest neighbor rules. *IEEE Trans. on Autom. Cont.*, 48(6):988–1001, 2003.

I. Kaminer, A. Pascoal, E. Hallberg, and C. Silvestre. Trajectory tracking for autonomous vehicles: An integrated approach to guidance and control. *AIAA Journal of Guidance, Control, and Dynamics*, 21(1), 1998.

I. Kaminer, O. Yakimenko, A. Pascoal, and R. Ghabcheloo. Path generation, path following and coordinated control for timecritical missions of multiple UAVs. *American Control Conference*, pages 4906 – 4913, June 2006.

I. Kaminer, O. Yakimenko, V. Dobrokhodov, A. Pascoal, N. Hovakimyan, V. V. Patel, C. Cao, and A. Young. Coordinated path following for time-critical missions of multiple UAVs via $\mathcal{L}_1$ adaptive output feedback controllers. *AIAA Guidance, Navigation and Control Conference, AIAA 2007-6409, Hilton Head Island, SC*, August 2007.

Y. Kim and M. Mesbahi. On maximizing the second smallest eigenvalue of state-dependent graph Laplacian. *IEEE Trans. on Autom. Cont.*, 51(1):116–120, 2006.

Z. Lin, B. Francis, and M. Maggiore. State agreement for coupled nonlinear systems with time-varying interaction. *SIAM Journal of Control and Optimization*, 2005. in review.

Z. Lin, B. Francis, and M. Maggiore. State agreement for continuous-time coupled nonlinear systems. *SIAM Journal of Control and Optimization*, 46 (1):288–307, 2007.

M. Mesbahi. On state-dependent dynamic graphs and their controllability properties. *IEEE Trans. on Autom. Cont.*, 50(3):387–392, 2005.

M. Mesbahi and F. Hadaegh. Formation flying control of multiple spacecraft via graphs, matrix inequalities, and switching. *AIAA Journal of Guidance, Control, and Dynamics*, 24(2):369–377, 2001.

R. Sepulchre, D. Paley, and N. Leonard. Collective motion and oscillator synchronization. In *Proc. of Block Island Workshop on Cooperative Control*, pages 189–205, Block Island, RI, 2003.

D. Soetanto, L. Lapierre, and A. Pascoal. Adaptive, non-singular path following, control of dynamic wheeled robots. In *Proc. ICAR*, Coimbra, Portugal, 2003.

Y. Song, Y. Li, and X. Liao. Orthogonal transformation based robust adaptive close formation control of multi-UAVs. In *Proc. of American Control Conf.*, pages 2983–2988, Portland, OR, 2005.

D. Stilwell and B. Bishop. Platoons of underwater vehicles. *IEEE Control Systems Magazine*, 20(6):45–52, Dec. 2000.

D. Stilwell, E. Bollt, and D. Roberson. Sufficient conditions for fast switching synchronization in time-varying network topologies. *SIAM Journal of Applied Dynamical Systems*, 6(1):140–156, 2006.

D. Stipanovic, G. Inalhan, R. Teo, and C. Tomlin. Decentralized overlapping control of a formation of unmanned aerial vehicles. *Automatica*, 40(1):1285–1296, 2004.

V. Taranenko. *Experience of Ritz's, Puankare's and Ljapunov's Methods Utilization for Flight Dynamics Tasks Solution.* Air Force Engineering Academy Press, 1986.

J. Tsitsiklis and M. Athans. Convergence and asymptotic agreement in distributed decision problems. *IEEE Transaction on Autom. Cont.*, 29(1): 42–50, 1984.

O. Yakimenko. Direct method for rapid prototyping of near-optimal aircraft trajectories. *AIAA Journal of Guidance, Control, & Dynamics*, 23(5):865–875, 2000.